The Search for Magnetotail Twisting at Mercury: Comparing MESSENGER Observations with the Terrestrial Case

N. Romanelli[1,2], G. A. DiBraccio[2], J. Slavin[3], C. Bowers[3], T. Weber[2,4]

[1]Department of Astronomy, University of Maryland, College Park, MD, USA.
[2]Planetary Magnetospheres Laboratory, NASA Goddard Space Flight Center, Greenbelt, MD, USA.
[3]Department of Climate and Space Sciences and Engineering, University of Michigan, Ann Arbor, MI, USA.
[4]Howard University, Department of Physics and Astronomy, Washington DC, USA.

Key Points:

- We find an upper bound for Mercury's near tail twist of ∼3 degrees, in association with the IMF dawn-dusk (By) component.
- The IMF By is able to affect Mercury's magnetotail current sheet and the local dipolar field can partly explain the small twist.
- Comparisons with observations from Earth suggest the tail twist could be detectable by Bepi-Colombo further downstream of Mercury.

Corresponding author: Norberto Romanelli, norberto.romanelli@nasa.gov, https://orcid.org/0000-0001-9210-0284

Abstract

Previous studies reported that the terrestrial and Martian magnetotails can become twisted due to the solar wind-planetary interaction; however, the associated physical processes proper of intrinsic and induced magnetospheres are still under debate. In particular, there is evidence that the Interplanetary Magnetic Field (IMF) dawn-dusk component (By) plays a major role in both environments, affecting the sense of twist. Here, we analyze all MESSENGER Magnetometer observations to investigate the IMF By influence on Mercury's magnetotail. We find that Mercury's tail twist is very small ($\lesssim$3 degrees), for a median downtail distance of ∼2 Mercury radii. We also identify a correlation between the IMF By and the local By component around the magnetotail current sheet. These results suggest the small (or lack of) twist may be explained by the dipolar field strength in the near-magnetotail. We examine this hypothesis by putting these observations into context with studies on the terrestrial magnetotail.

Plain Language Summary

Previous studies identified a twist in the magnetotail structures on Earth and Mars. This twist is affected by the dawn-dusk component (By) of the background magnetic field convected by the solar wind. To improve the current understanding of these phenomena, we analyze all MESSENGER magnetic field data in Mercury's magnetotail. We find an upper bound for the tail twist of ∼3 degrees, based on observations obtained centered at ∼ 2 Mercury radii downstream from the planet. Our results suggest the small (or lack of) twist at Mercury could be understood in terms of the dipolar field strength in the magnetotail region near the planet. We put these observations into context with conclusions reported at the terrestrial magnetotail and argue the Bepi-Colombo mission may see a more developed twist, as the planned apoapsis is expected to be further downtail from Mercury, compared to MESSENGER.

1 Introduction

Mercury, the smallest and innermost planet in the solar system, possesses an intrinsic, relatively weak (∼195 nT R_M^3, with 1 R_M ∼ 2440 km), global magnetic field (Ness et al., 1974; Anderson et al., 2011). This field is highly dipolar, with a moment that is closely aligned with its rotation axis (dipole tilt $\leq$ 0.8°) and offset ∼ 0.2 R_M northward from the planet's center (Anderson et al., 2007, 2011, 2012; Johnson et al., 2012). The interaction between Mercury's magnetic field and the high solar wind pressure in the inner heliosphere generates a small magnetosphere whose mean magnetopause standoff distance is ∼ 1.45 R_M(Philpott et al., 2020), shielding the planet's surface from the solar wind most of the time (J. A. Slavin et al., 2014, 2019; Winslow et al., 2020).

Mercury is also characterized by an iron-rich, electrically conducting core with a large radius of ∼ 0.8 R_M (Smith et al., 2012; Hauck et al., 2013; Katsura et al., 2021). The presence of this core implies the electromagnetic coupling between Mercury's interior and its plasma environment can play an important role in the solar wind-magnetosphere interaction (e.g., Hood & Schubert, 1979). Indeed, variability of magnetic flux at the core can result in significant eddy currents, whose associated magnetic field can be an appreciable fraction of the planetary dipolar field (e.g., Glassmeier et al., 2007; Saur et al., 2010; J. A. Slavin et al., 2014; Jia et al., 2015; Heyner et al., 2016; Johnson et al., 2016; Jia et al., 2019; Wardinski et al., 2019; Zhong, Wan, Wei, et al., 2015).

The solar wind along Mercury's orbit is partly defined by low Alfvenic Mach numbers and plasma beta values, due to the planet's proximity to the Sun. Thus, it presents favorable conditions for magnetic reconnection between the shocked Interplanetary Magnetic Field (IMF) and the planet's intrinsic magnetic field (e.g., J. A. Slavin & Holzer, 1981; Gershman et al., 2013; James et al., 2017; Romanelli, DiBraccio, Gershman, et al.,

2020; Zurbuchen et al., 2004; DiBraccio et al., 2013; J. A. Slavin et al., 2009, 2012). Indeed, DiBraccio et al. (2013) found that magnetopause reconnection can occur under most magnetic shear angles between the IMF and the planetary field and with high dimensionless reconnection rates (0.15 ± 0.02). These rates are a factor ~ 3 larger than values reported at Earth, the only other known planetary magnetosphere with dynamics dominated by a reconnection-driven Dungey-cycle (Dungey, 1961). This cycle of magnetic flux and plasma circulation begins with magnetopause reconnection, creating open magnetic field lines that are then convected to the magnetotail. This magnetic flux eventually reconnects within the tail and returns to Mercury's dayside on $\sim 3-3.5$ min timescales (e.g., Dungey, 1961; DiBraccio et al., 2013; J. A. Slavin et al., 2009, 2012; Imber & Slavin, 2017; J. A. Slavin et al., 2021).

Spacecraft observations and numerical simulations have also enabled characterizing Mercury's magnetosphere's global response to varying IMF orientations, and its implications for several processes, including magnetic reconnection (e.g., Aizawa et al., 2021; Jia et al., 2015, 2019; Richer et al., 2012). For example, in a cross-comparison global simulation model effort, Aizawa et al. (2021) examined the locations of reconnection sites under a configuration with purely northward IMF configuration. In addition, Jia et al. (2015, 2019) reported Mercury's magnetosphere exhibits strong asymmetries with respect to the planetary equatorial plane, which are attributed to its dipole offset and the large solar wind flow aligned IMF component, typically present in the solar wind upstream of this planet. These asymmetries not only modify the magnetopause and magnetotail current systems, but can also affect the location of the magnetotail reconnection X-line.

Studies on the terrestrial magnetosphere show that the IMF orientation at the time of magnetopause reconnection affects the transfer of solar wind momentum and energy into the system and can impact, for instance, the magnetotail configuration (e.g., Cowley, 1981; Fedder et al., 1991, 1995; Luhmann et al., 1984; Tsyganenko et al., 2015; Pitknen et al., 2021). One of the most noteworthy effects is the magnetotail current sheet rotation or twisting dependence on the IMF dawn-dusk component (By). The current sheet is observed to rotate counter-clockwise in the cross-sectional tail plane (looking from Earth toward the tail) for duskward, IMF By> 0. The tail rotates clockwise for dawnward, IMF By< 0 (e.g., Kaymaz et al., 1994; Owen et al., 1995; Tsyganenko et al., 1998, 2015; Xiao et al., 2016; Sibeck et al., 1985; Tenfjord et al., 2015). Additionally, several statistical analyses indicate that the magnetotail current sheet rotation increases with downtail distance and the IMF By magnitude (e.g., Kaymaz et al., 1994; Tsyganenko et al., 2015). There are also indications of asymmetries in the degree of magnetotail twisting depending on the polarity of the IMF By and Bz components (e.g., Kaymaz et al., 1994; Pitknen et al., 2021).

Cowley (1981) developed a theoretical model that seeks to explain some of the properties of the terrestrial tail twist. The presence of a non-zero IMF By component generates asymmetric dayside magnetopause reconnection, affecting the magnetic flux loading in the magnetotail lobes (e.g., Gosling et al., 1985; Khurana et al., 1996; Park et al., 2006; Tenfjord et al., 2015). Under these conditions, this model proposes that tangential stresses on the tail magnetopause by the deflecting open magnetic field lines exert a torque on the magnetotail lobes that is responsible for the current sheet rotation (Cowley, 1981).

Interestingly, although Mars lacks an intrinsic global magnetic field, DiBraccio et al. (2018) discovered a magnetotail twist in its hybrid magnetosphere (Acuña et al., 1998). The observed tail twist at Mars is also dependent on the IMF By component and responds with the same sense as that of Earth's. Therefore, it has been suggested that the Martian tail twist could be associated with magnetic field reconnection between the shocked IMF and remnant crustal magnetic fields (Acua et al., 1999; DiBraccio et al., 2018). Moreover, a statistical study on the factors that influence the Martian magnetotail twisting shows that the rather large twist (compared to the terrestrial case) increases with down-

tail distance to Mars and is also larger for duskward IMF By orientation (DiBraccio et al., 2022).

While studies have been devoted to understanding magnetotail twists at Earth's and Mars' magnetospheres, there are still several open questions. The physical mechanisms behind these tail rotations are not sufficiently well determined and, therefore, the properties that the planetary obstacle and the solar wind must meet to do so. For example, Earth and Mars have different planetary atmospheric and magnetic environments (i.e., global and crustal fields) with distinct spatial and temporal scales that experience different solar wind parameters at their location in the heliosphere. For this reason, assessing whether a tail twist is present within another intrinsic magnetosphere will help to better understand the forces at play. In this work, we seek to contribute to the current understanding of this topic by performing the first analysis of Mercury's magnetotail configuration as a function of the IMF dawn-dusk component in the search for a potential twist, based on all MErcury, Surface, Space ENvironment, GEochemistry and Ranging (MESSENGER) magnetic field observations. We also analyze the extent to which magnetic field observations in the near-magnetotail of Mercury present signatures correlated with the IMF By and the planetary dipolar field. Finally, we put this study into context with previous reports on the terrestrial magnetotail.

2 Data and Selection Criteria

On 18 March 2011, MESSENGER began its orbit around Mercury. The initial spacecraft orbit had a period of $\sim$ 12 hours and high eccentricity (apoapsis altitude of $\sim$ 6.1 R_M) (Solomon et al., 2007). Equipped with a three-axis, ring-core, fluxgate Magnetometer (MAG), MESSENGER provided in-situ magnetic field measurements at a 20 Hz sampling rate (Anderson et al., 2007). On 16 April 2012, the spacecraft's apoapsis altitude was reduced to $\sim$ 4.1 R_M, resulting in an orbital period of $\sim$8 hr and providing a clearer picture of Mercury's magnetosphere, particularly between the subsolar magnetopause region to $\sim 3\,R_M$ downtail. MESSENGER's mission ended on 30 April 2015 (e.g., J. A. Slavin et al., 2019).

In this work, we analyze all MESSENGER MAG data by applying the following methodology: we compute 10 s magnetic field averages, as this resolution is sufficient for assessing large-scale trends within the magnetotail. We identify and select MESSENGER's orbits that sampled both the region upstream from Mercury's bow shock and the Hermean magnetotail. For this, we make use of the bow shock crossing list reported by Philpott et al. (2020). For each of these MESSENGER orbits, we estimate the IMF associated with magnetic field observations in the magnetotail as the average between the inbound and outbound IMF estimates for the same orbit. These are computed based on a 10 minute magnetic field average upstream from Mercury's bow shock.

Magnetic field data is analyzed in aberrated Mercury Solar Magnetic (MSM) coordinates. This coordinate system is centered on Mercury's (offset) magnetic field dipole and takes into account the planet's orbital velocity around the Sun (Anderson et al., 2011). The X_{MSM} axis points sunward along the Sun-Mercury direction, the Y_{MSM} axis is antiparallel to Mercury's orbital velocity and the Z_{MSM} completes the right-handed system. The aberration angle varies between $\sim$ 5.6° and $\sim$ 8.4°, due to Mercury's highly eccentric orbit.

Lastly, the selection criteria also considers the magnetotail region sampled by MESSENGER. Hereafter, we present our results analyzing all MAG measurements inside the nominal magnetopause of Mercury, and downstream of the $X_{MSM} = -1.22\,R_M$ plane, where the inner edge of the magnetotail current sheet is located (Zhong, Wan, Slavin, et al., 2015; Philpott et al., 2020; Poh et al., 2017). However, we note the presented re-

sults do not change significantly if consider a smaller threshold, i.e., further away from the planet.

Figure 1a-c displays MESSENGER position inside the magnetotail of Mercury, downstream from the $X_{MSM} = -1.22\,R_M$ plane. This data-set has a median $X_{MSM} = -1.91\,R_M$ and a standard deviation equal to $0.57\,R_M$. The spacecraft mostly explored the southern magnetotail lobe throughout the mission, but also sampled the magnetotail current sheet and the near northern lobe (Poh et al., 2017; Rong et al., 2018). Figure 1d-f show the observed distributions of the IMF properties for the corresponding MESSENGER orbits. The IMF strength ranged between ∼14.0 and ∼24.3 nT (lower and upper quartiles) with a median equal to ∼18.5 nT. The IMF clock and cone angles distributions show the IMF is mainly contained in the ecliptic plane with IMF clock angle maximum occurrences near ~ -75 and ~ 95 degrees (Figure 1e), and quasi-radial with an IMF Parker spiral angle peaking at about ~ -20 and ~ 165 degrees (Figure 1f). These distributions are consistent with nominal values along Mercury's orbit around the Sun.

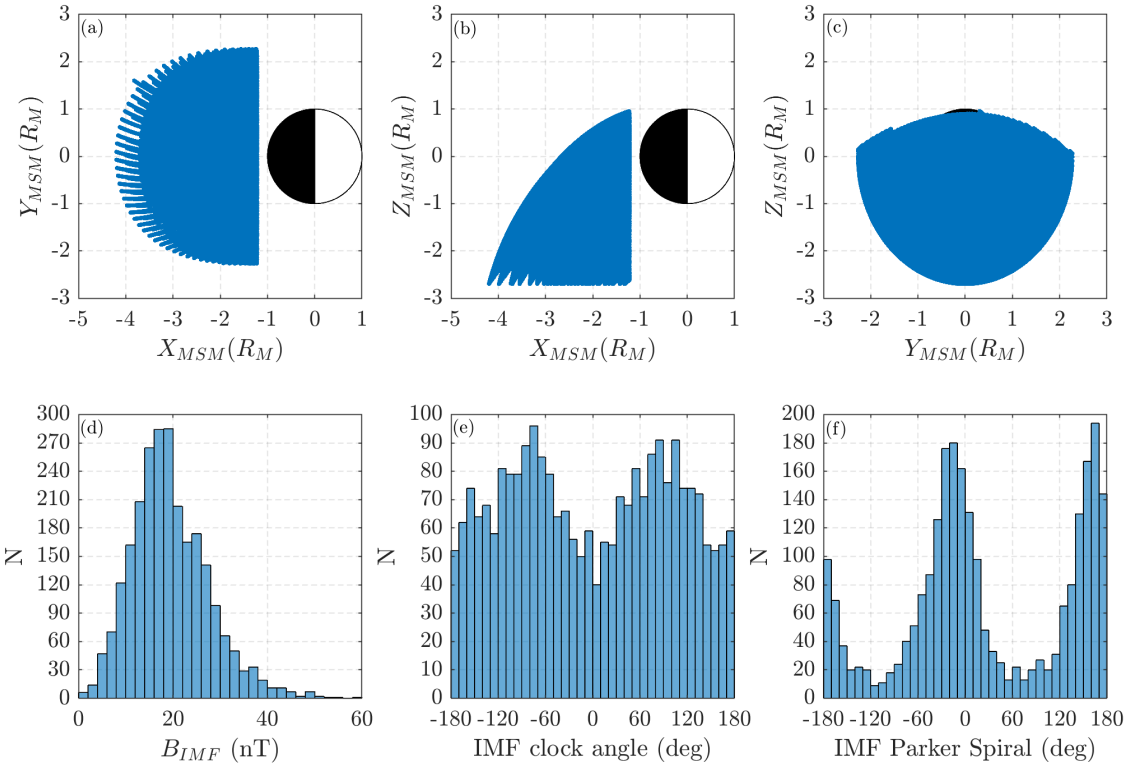

Figure 1. (a–c) MESSENGER position in Mercury's magnetotail ($X_{MSM} \leq -1.22\,R_M$) for orbits considered into this study. Views are displayed (a) in the equatorial plane, (b) in the meridional plane, and (c) from Mercury toward the magnetotail. (d–f) Distributions of MESSENGER magnetic field observations are shown for (d) IMF strength, (e) IMF clock angle, and (f) IMF Parker spiral angle.

3 Results and Discussion

Figure 2a-b display the cross-tail projection in the Y_{MSM}-Z_{MSM} plane of the mean Bx component in Mercury's magnetotail (color-coded), for IMF By<0 and By>0, re-

spectively. As described in the Introduction, this IMF component is found to affect the magnetotail lobes location in the terrestrial and Martian magnetospheres (e.g., Kaymaz et al., 1994; DiBraccio et al., 2018). Initially, we note the current sheet is observed near the $Z_{MSM} = 0\,R_M$ plane (white region between the red and blue lobes in Figure 2), regardless of the IMF By polarity. Given the horizontal appearance of the current sheet at $Z_{MSM} = 0\,R_M$ across the full width of Mercury's tail, the magnetotail twist is small, if present, at these downtail distances sampled by MESSENGER. This Figure also shows that Mercury's offset dipole results in a $\sim 0.2R_M$ shift of the current sheet northward from the planetary equator, which is taken into account in the definition of the MSM coordinate system. To determine whether a twist may exist within Mercury's tail and provide an estimation of its inclination, we apply a similar methodology to Romanelli et al. (2018, 2019); DiBraccio et al. (2022), that consists in finding the tail lobe center.

In our case, we focus the analysis in estimating the geometric center of the southern tail lobe. The northern lobe is not considered in this computation since there is not adequate coverage based on MESSENGER's orbital geometry. As shown in Romanelli et al. (2018, 2019); DiBraccio et al. (2022), the direction defined by the center of the magnetic map, [Y_{MSM}, Z_{MSM}]=[0,0] R_M and the center of the tail lobe is roughly perpendicular to the average current sheet location. The computation of the geometric center is based on all bins inside the nominal magnetopause boundary (Zhong, Wan, Slavin, et al., 2015; Philpott et al., 2020) with a negative mean Bx (southern hemisphere), based on at least five MESSENGER orbits (c-d). Given that the solar wind conditions vary with time, each MESSENGER orbit is considered an independent sampling of Mercury's magnetotail. Our results suggest the southern magnetotail lobe may be twisted by ~ 1.5 degrees clockwise (counterclockwise) for negative (positive) IMF By, seen from Mercury towards the tail (view in Figure 2a-d). These results do not change significantly if the tail twist is estimated based on the median Bx component magnetic field maps, for the resolution that can be achieved with the current data set (bin size of $0.1R_M \times 0.1R_M$). In addition, we also report that the tail twist estimates do not change significantly if we consider MESSENGER orbits where the inbound and outbound IMF estimates are less than 45 and 90 degrees apart, where the IMF is more likely to be stable. These cases correspond to $\sim 42\%$ and $\sim 87\%$ of the MESSENGER orbits (2484) considered in the bin maps shown in Figure 2, respectively.

These magnetotail twist estimates have an uncertainty on the same order (~ 1.5 degrees), due to the considered magnetic maps spatial resolution. These results therefore suggest Mercury's tail may be twisted up to ~ 3 degrees clockwise (counterclockwise) for negative (positive) IMF By (seen from the planet towards the magnetotail tail). Nevertheless, they do not rule out the possibility of a lack of twist in this region of the Hermean magnetotail.

Following this characterization of the Hermean magnetotail, Figure 3a indicates there is a linear correlation ($R \sim 0.33$) between By around Mercury's tail current sheet (MAG data with $|Bx| < 0.01B$ and $|Z_{MSM}| < 0.2\,R_M$), and the associated IMF By component for the same MESSENGER orbit. These observations suggest the IMF is able to affect Mercury's magnetotail structure to some extent. In addition, Figure 3b shows that the absolute values of the lower and upper quartiles of the By distribution (extremes of the black bars) are on the order of $\sim 2-3$ nT for $X_{MSM} > -2R_M$, taking values much lower than Bz around the current sheet (red vertical bars). The latter decreases as a function of $-X_{MSM}$, as the distance from Mercury's dipole increases. If we consider the local By and Bz components are a proxy for the IMF By and Mercury's dipolar influence on the tail, respectively, Figure 3b suggests the dipole magnetic field is strong enough to reduce/prevent tail twisting in the near-magnetotail of Mercury.

To examine the hypothesis that Mercury's tail may become more twisted farther from the planet as the dipole magnetic field's influence decreases, we put our results into context with previous studies on the terrestrial magnetotail. The Earth's magnetotail

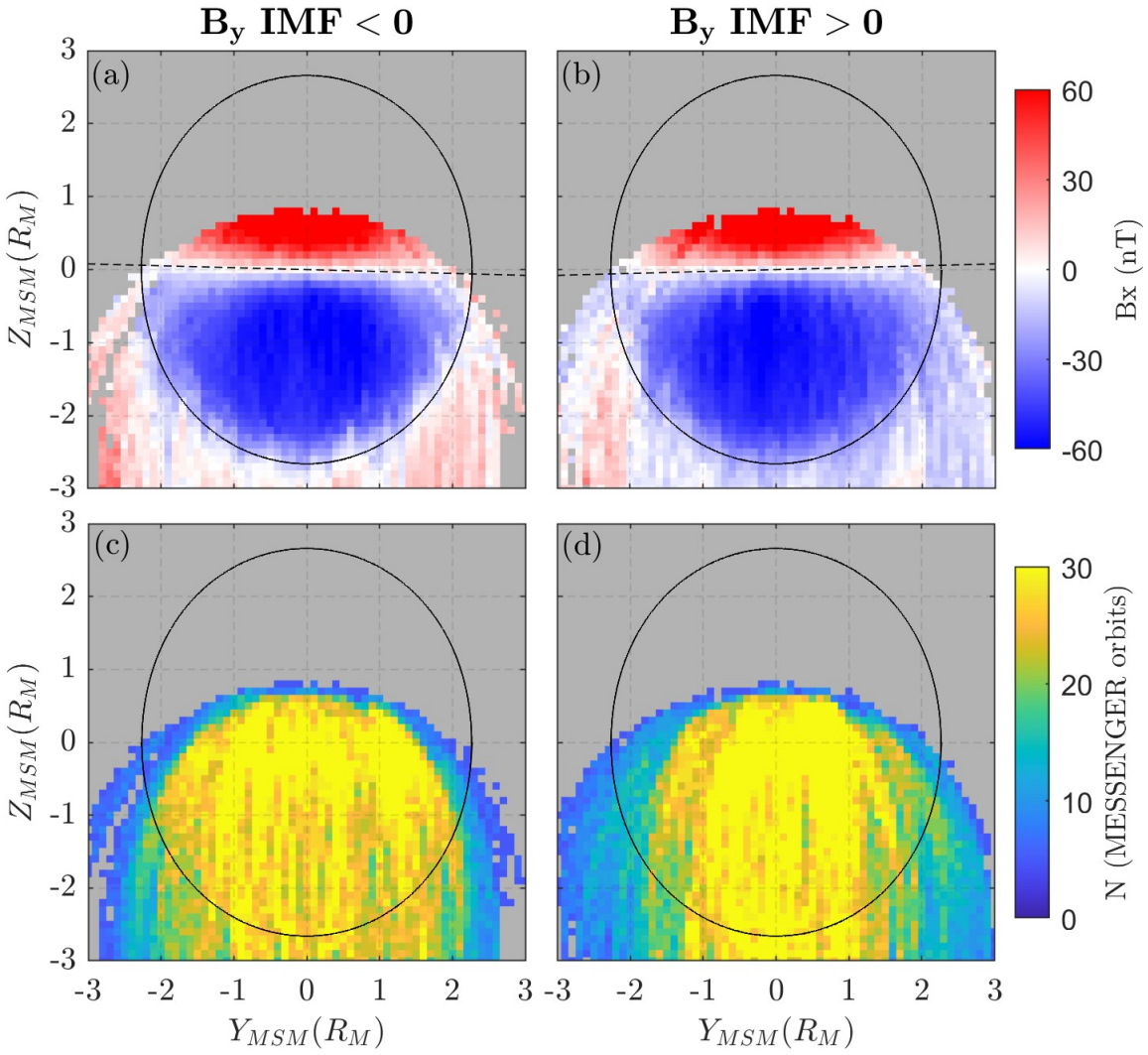

Figure 2. (a-b) Cross-tail projections of the mean Bx component in the Hermean magnetotail as a function of the aberrated Y_{MSM} and Z_{MSM} coordinates, based on MESSENGER Magnetometer observations downstream from the X_{MSM}=−1.22 R_M plane. The tail structure under periods of negative and positive IMF By is shown in panels a and b, respectively. The red and blue colors display the local +Bx and -Bx components, respectively. These correspond to sunward (out of the page) and antisunward (into the page) directions, respectively. The dashed black lines display the estimated current sheet twists, based on the computed geometric center of the southern magnetotail lobe. (c-d) Number of MESSENGER orbits per bin associated with the magnetic maps shown in panels (a) and (b), respectively. The black curves correspond to the average magnetopause location at $X_{MSM} = -2\,R_M$, and are shown for reference (Zhong, Wan, Slavin, et al., 2015).

is the most studied case and likely the closest environment to that of Mercury's. Indeed, the Dungey cycle dominates the dynamics of both magnetospheres created by the interaction of the solar wind with planetary magnetic dipole fields. Figure 4 presents a comparison between our tail twist estimation at Mercury and several statistical studies using magnetic field data from observations at Earth. Firstly, we note that the terrestrial

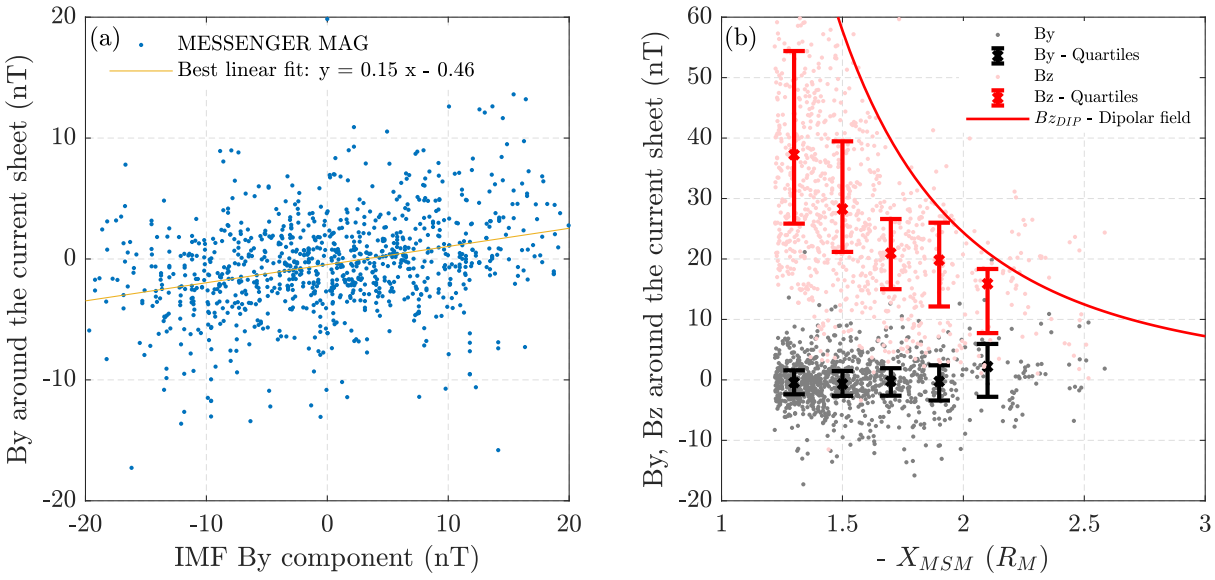

Figure 3. (a) By around Mercury's magnetotail current sheet as a function of the average IMF By component upstream from the bow shock for the same MESSENGER orbit. The yellow curve displays the best linear fit. (b) By and Bz around Mercury's magnetotail current sheet as a function of the downtail distance (in grey and pink, respectively). Black and red vertical bars span the 25th to the 75th percentiles of the gray and pink data sets, respectively, within each bin (0.2 R_M width). The middle point in each bar corresponds to the associated median. For reference, the red solid curve shows the Bz component of Mercury's dipolar field around the current sheet (Bz_{DIP}).

tail twist is ~ 3 degrees (or smaller) for a downtail distance of $X = 20 - 22\,R_E$ (R_E stands for Earth's radii). At these distances, the Earth's magnetic field dipole Bz component at the magnetotail current sheet (Bz_{DIP}) is ~ 3 nT. Considering that the average By at the terrestrial current sheet ranges between ~ 0.25 and 0.5 the upstream By IMF (~ 4 nT) (see Table 1, Kaymaz et al., 1994), we observe the tail twist becomes noticeable when the local By ($\sim 1{-}2$ nT) is on the order of Bz_{DIP}. These results suggest the terrestrial twist is appreciable when the influence of the IMF By in the current sheet is on the order of the local planetary dipole field strength (Bz_{DIP}).

Figure 4 also shows an overall increase in terrestrial tail twist with downtail distance and By IMF intensity. In particular, magnetic field observations of tail current sheet twist up to a downtail distance of 60 R_E were fitted with a function linearly dependent on the IMF By (see last term in Equation 3 in Tsyganenko et al., 2015). The best fits are shown as a function of downtail distance (for the zero dipole tilt angle case) for three representative values of the IMF By by means of the dashed yellow lines in Figure 4 (see considered coefficients in Table 1, Tsyganenko et al. (2015)).

If we apply the previous considerations to the Hermean magnetotail case, we find the dipolar field Bz component at the current sheet (Bz_{DIP}) is on the order of 4 nT for $X \sim 3.6\,R_M$. The 4 nT reference denotes the standard deviation of By in Mercury's current sheet for all data analyzed (see Figure 3a). The computed critical distance is $\sim$ 1 Mercury radii further downstream than most of the MESSENGER data available for this study, providing an explanation for the relatively small observed (or lack of) tail twist. We also note that this value is within the BepiColombo Mercury Magnetospheric Or-

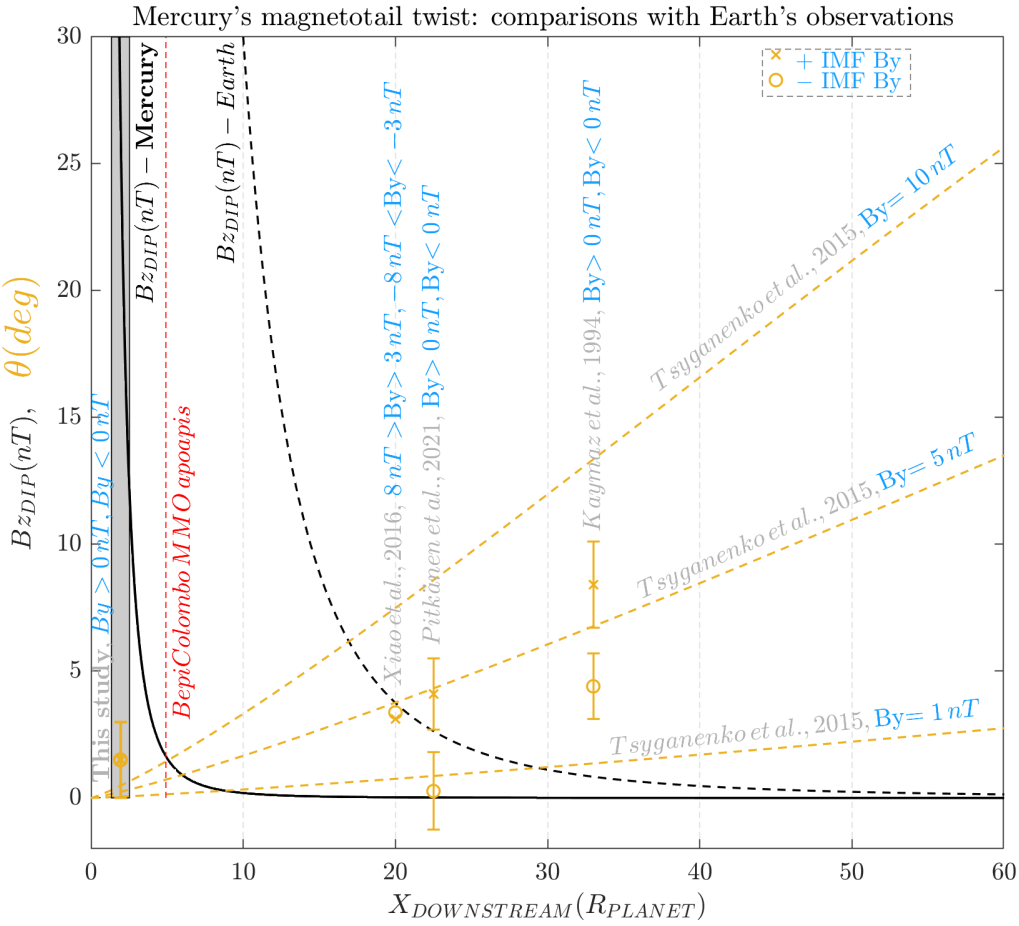

Figure 4. Comparison of our results with observations at the terrestrial magnetotail. Vertical axis shows the Bz component associated with Mercury's and Earth's magnetic dipoles at the respective magnetotail current sheet (black solid and dashed curves, respectively) and the observed tail twist (in yellow) for positive (cross) and negative (circle) IMF By (in light blue), as a function of the distance downstream from the planet (normalized with the planet's radii). Dash yellow lines correspond to the expected terrestrial tail twist for different IMF By intensities based on data fits reported by Tsyganenko et al. (2015). References and IMF By selection criteria associated with the corresponding papers are shown in grey and light blue, respectively. For instance, the yellow cross and circle shown at X=33 R_E, correspond to computed Earth's tail twist rotation for IMF $By > 0$ nT and $By < 0$ nT, respectively, according to Kaymaz et al. (1994).

biter (MMO) expected apoapsis ($\sim 4.9 R_M$). Thus, these results suggest this mission will not only be able to further characterize Mercury's magnetotail morphology and its dependence on the IMF, but it may also reveal a more developed tail twist, if present.

Previous studies also indicate that the terrestrial tail twist exhibits an asymmetrical behavior with a larger rotation under positive IMF By than under negative cases (Kaymaz et al., 1994; Owen et al., 1995; Pitknen et al., 2021). This preference for +IMF By was also observed at Mars (DiBraccio et al., 2022). Nevertheless, other works have not observed this trend (e.g., Xiao et al., 2016). Such asymmetry is also absent in Cowley (1981) and Tsyganenko et al. (2015) analytical models. Here, we report that our results

do not display signatures of this asymmetry in the near-magnetotail of Mercury. However, this could be detected by Bepi-Colombo further downstream of Mercury for a potentially more developed twist.

It is also worth emphasizing that the physical processes responsible for tail twist likely depend on more variables than the planetary dipole field and the IMF By component. For instance, Owen et al. (1995) reported a larger terrestrial tail twist for positive IMF Bz, suggesting that higher reconnection rates may reduce the current sheet rotation. Thus, although the By IMF at Mercury is typically $\sim 2{-}3$ times larger than that at Earth, the higher reconnection rates and wider magnetic shear angles under which magnetopause reconnection takes place potentially contribute to a smaller tail twist (DiBraccio et al., 2013; James et al., 2017; Romanelli & DiBraccio, 2021). Another potentially important factor is the IMF cone angle. In particular, the presence of a significant IMF Bx component could affect the reconnection sites location on the dayside magnetopause and thus the magnetic field loading in the magnetotail (see, e.g., Luhmann et al., 1984). Moreover, Mercury has no ionosphere but a rather large conductive core (see, e.g., Sun et al., 2021). This key difference does not only affect field aligned currents closure (J. Slavin et al., 1997; Anderson et al., 2014, 2018), but suggests fields induced at the core can increase Mercury's intrinsic dipolar field and therefore affect the degree to which the tail is twisted (Glassmeier et al., 2007). In this regard, we report a difference in the fraction of the IMF By value MESSENGER detects in Mercury's magnetotail. Indeed, Figure 3a suggests a ratio on the order 0.15 (slope associated with the linear fit), while studies at Earth detect values that are between 2 and 4 times larger (e.g., Kaymaz et al., 1994; Wing et al., 1995). This could be partly be due to the differences in the solar wind conditions upstream of Mercury and Earth and the intrinsic properties of these planets.

Finally, it is worth mentioning that the observed magnetotail twist at Mars is between $\sim$20° and $\sim$60°, for a ~ 2 Martian radii downtail distance. It displays variability with local time and Martian season and could be associated with magnetic reconnection between the IMF and crustal magnetic fields (DiBraccio et al., 2022). In addition, such a large tail twist may also result from the lack of a global dynamo-generated planetary dipole field. Indeed, asymmetries in the Martian current system (Dubinin et al., 2014b, 2014a; Ramstad et al., 2020), the shocked solar wind flow deflection (Dubinin et al., 2018; Romanelli et al., 2019; Romanelli, DiBraccio, Halekas, et al., 2020), and the IMF morphology around Mars (Crider et al., 2004; Brain et al., 2006; Romanelli et al., 2014, 2015) may also be contributing factors.

4 Conclusions

In this work we analyze the effects that the IMF dawn-dusk component has on the Hermean magnetotail and current sheet, based on all MESSENGER Magnetometer observations. Firstly, we determine an upper limit for Mercury's near-magnetotail ($\sim 2R_M$ downtail distance) small twist of $\sim$3° with the current sheet rotating clockwise (counterclockwise) for negative (positive) IMF By, seen from Mercury towards the tail. These estimates do not exclude the possibility of a lack of twist in this region. Secondly, we identify a linear correlation between By around Mercury's magnetotail current sheet and the associated IMF By component for the same MESSENGER orbit. We also find that the Bz component near the current sheet is much larger than By for the region explored, suggesting the planetary dipole magnetic field is sufficiently strong to limit or prevent twisting in Mercury's near-magnetotail. Finally, we find this interpretation is consistent with statistical studies focused on the Earth magnetotail and argue that, if present, a more developed twist could be observed by Bepi-Colombo given the planned apoapsis.

Overall, this study contributes to improving the current understanding of planetary magnetotail twists, which has currently been explored around three of the telluric planets (see, e.g., Tsyganenko et al., 2015; DiBraccio et al., 2022). We note variations

in the tail twist at two Dungey cycle-driven intrinsic magnetospheres and a relatively large twist in Mars's hybrid magnetosphere. To better determine the physical processes at play in intrinsic and induced magnetospheres, future works would benefit from further analysis of the Hermean magnetosphere based on Bepi-Colombo observations and exploration of the induced magnetotail of Venus. Moreover, numerical simulations of Mercury's magnetosphere for different solar wind and IMF configurations (e.g., perihelion and aphelion conditions) can help improving the current understanding on this matter (see, e.g., Jia et al., 2015). In particular, they can provide valuable information to determine conditions favorable for magnetotail twisting, the location where this effect would be noticeable and how it may develop with downtail distance.

Acknowledgments

The material is based upon work supported by NASA under award number 80GSFC21M0002. N.R. and G.A.D. were also supported by the NASA ROSES Solar System Workings program (NNH19ZDA001N-SSW) under proposal #19-SSW19-0106.

5 Open Research

Data Availability Statement

MESSENGER MAG data used in this study are publicly available through the Planetary Data System (`https://pds-ppi.igpp.ucla.edu/search/view/?f=yes&id=pds://PPI/MESS-E_V_H_SW-MAG-3-CDR-CALIBRATED-V1.0/DATA/MSO`).

References

Acuña, M. H., Connerney, J. E. P., Wasilewski, P., Lin, R. P., Anderson, K. A., Carlson, C. W., ... Ness, N. F. (1998). Magnetic Field and Plasma Observations at Mars: Initial Results of the Mars Global Surveyor Mission. *Science*, *279*(5357), 1676–1680. doi: 10.1126/science.279.5357.1676

Acua, M. H., Connerney, J. E. P., F., N., null Ness, Lin, R. P., Mitchell, D., ... Cloutier, P. (1999). Global distribution of crustal magnetization discovered by the mars global surveyor mag/er experiment. *Science*, *284*(5415), 790-793. Retrieved from `https://www.science.org/doi/abs/10.1126/science.284.5415.790` doi: 10.1126/science.284.5415.790

Aizawa, S., Griton, L., Fatemi, S., Exner, W., Deca, J., Pantellini, F., ... Usui, H. (2021). Cross-comparison of global simulation models applied to mercurys dayside magnetosphere. *Planetary and Space Science*, *198*, 105176. Retrieved from `https://www.sciencedirect.com/science/article/pii/S0032063321000155` doi: https://doi.org/10.1016/j.pss.2021.105176

Anderson, B. J., Acua, M. H., Lohr, D. A., Scheifele, J., Raval, A., Korth, H., & Slavin, J. A. (2007, August). The Magnetometer Instrument on MESSENGER. *Space Science Reviews*, *131*(1-4), 417–450. Retrieved 2021-08-30, from `http://link.springer.com/10.1007/s11214-007-9246-7` doi: 10.1007/s11214-007-9246-7

Anderson, B. J., Johnson, C. L., Korth, H., & Philpott, L. C. (2018, March). Birkeland Currents at Mercury: Review and Comparison With Earth. In A. Keiling, O. Marghitu, & M. Wheatland (Eds.), *Geophysical Monograph Series* (pp. 279–302). Hoboken, NJ, USA: John Wiley & Sons, Inc. Retrieved 2021-08-30, from `https://onlinelibrary.wiley.com/doi/10.1002/9781119324522.ch17` doi: 10.1002/9781119324522.ch17

Anderson, B. J., Johnson, C. L., Korth, H., Purucker, M. E., Winslow, R. M., Slavin, J. A., ... Zurbuchen, T. H. (2011, September). The Global Magnetic Field of Mercury from MESSENGER Orbital Observations. *Science*,

333(6051), 1859–1862. Retrieved 2021-08-31, from https://www.sciencemag.org/lookup/doi/10.1126/science.1211001 doi: 10.1126/science.1211001

Anderson, B. J., Johnson, C. L., Korth, H., Slavin, J. A., Winslow, R. M., Phillips, R. J., ... Solomon, S. C. (2014, November). Steady-state field-aligned currents at Mercury: Field-Aligned Currents at Mercury. *Geophysical Research Letters*, *41*(21), 7444–7452. Retrieved 2021-08-30, from http://doi.wiley.com/10.1002/2014GL061677 doi: 10.1002/2014GL061677

Anderson, B. J., Johnson, C. L., Korth, H., Winslow, R. M., Borovsky, J. E., Purucker, M. E., ... McNutt, R. L. (2012, December). Low-degree structure in Mercury's planetary magnetic field: MERCURY'S PLANETARY MAGNETIC FIELD. *Journal of Geophysical Research: Planets*, *117*(E12), n/a–n/a. Retrieved 2021-08-30, from http://doi.wiley.com/10.1029/2012JE004159 doi: 10.1029/2012JE004159

Brain, D. A., Mitchell, D. L., & Halekas, J. S. (2006). The magnetic field draping direction at mars from april 1999 through august 2004. *Icarus*, *182*(2), 464-473. Retrieved from https://www.sciencedirect.com/science/article/pii/S0019103505004902 (Results from the Mars Express ASPERA-3 Investigation) doi: https://doi.org/10.1016/j.icarus.2005.09.023

Cowley, S. (1981, January). Magnetospheric asymmetries associated with the y-component of the IMF. *Planetary and Space Science*, *29*(1), 79–96. Retrieved 2021-08-30, from https://linkinghub.elsevier.com/retrieve/pii/0032063381901410 doi: 10.1016/0032-0633(81)90141-0

Crider, D. H., Brain, D. A., Acuña, M. H., Vignes, D., Mazelle, C., & Bertucci, C. (2004). Mars global surveyor observations of solar wind magnetic field draping around mars. In D. Winterhalter, M. Acuña, & A. Zakharov (Eds.), *Mars' magnetism and its interaction with the solar wind* (pp. 203–221). Dordrecht: Springer Netherlands. Retrieved from https://doi.org/10.1007/978-0-306-48604-3_5 doi: 10.1007/978-0-306-48604-3_5

DiBraccio, G. A., Luhmann, J. G., Curry, S. M., Espley, J. R., Xu, S., Mitchell, D. L., ... Jakosky, B. M. (2018, May). The Twisted Configuration of the Martian Magnetotail: MAVEN Observations. *Geophysical Research Letters*, *45*(10), 4559–4568. Retrieved 2021-08-30, from http://doi.wiley.com/10.1029/2018GL077251 doi: 10.1029/2018GL077251

DiBraccio, G. A., Romanelli, N., Bowers, C. F., Gruesbeck, J. R., Halekas, J. S., Ruhunusiri, S., ... Curry, S. M. (2022). A statistical investigation of factors influencing the magnetotail twist at mars. *Geophysical Research Letters*, *49*(12), e2022GL098007. Retrieved from https://agupubs.onlinelibrary.wiley.com/doi/abs/10.1029/2022GL098007 (e2022GL098007 2022GL098007) doi: https://doi.org/10.1029/2022GL098007

DiBraccio, G. A., Slavin, J. A., Boardsen, S. A., Anderson, B. J., Korth, H., Zurbuchen, T. H., ... Solomon, S. C. (2013, March). MESSENGER observations of magnetopause structure and dynamics at Mercury: MAGNETOPAUSE RECONNECTION AT MERCURY. *Journal of Geophysical Research: Space Physics*, *118*(3), 997–1008. Retrieved 2021-08-30, from http://doi.wiley.com/10.1002/jgra.50123 doi: 10.1002/jgra.50123

Dubinin, E., Fraenz, M., Ptzold, M., Halekas, J. S., Mcfadden, J., Connerney, J. E. P., ... Zelenyi, L. (2018). Solar wind deflection by mass loading in the martian magnetosheath based on maven observations. *Geophysical Research Letters*, *45*(6), 2574-2579. Retrieved from https://agupubs.onlinelibrary.wiley.com/doi/abs/10.1002/2017GL076813 doi: https://doi.org/10.1002/2017GL076813

Dubinin, E., Fraenz, M., Zhang, T. L., Woch, J., & Wei, Y. (2014a). Magnetic fields in the mars ionosphere of a noncrustal origin: Magnetization features. *Geophysical Research Letters*, *41*(18), 6329-6334. Retrieved from https://agupubs.onlinelibrary.wiley.com/doi/abs/10.1002/2014GL061453 doi:

https://doi.org/10.1002/2014GL061453

Dubinin, E., Fraenz, M., Zhang, T. L., Woch, J., & Wei, Y. (2014b). Magnetic fields in the venus ionosphere: Dependence on the imf directionvenus express observations. *Journal of Geophysical Research: Space Physics*, *119*(9), 7587-7600. Retrieved from https://agupubs.onlinelibrary.wiley.com/doi/abs/10.1002/2014JA020195 doi: https://doi.org/10.1002/2014JA020195

Dungey, J. W. (1961, Jan). Interplanetary magnetic field and the auroral zones. *Phys. Rev. Lett.*, *6*, 47–48. Retrieved from https://link.aps.org/doi/10.1103/PhysRevLett.6.47 doi: 10.1103/PhysRevLett.6.47

Fedder, J. A., Lyon, J. G., Slinker, S. P., & Mobarry, C. M. (1995). Topological structure of the magnetotail as a function of interplanetary magnetic field direction. *Journal of Geophysical Research: Space Physics*, *100*(A3), 3613-3621. Retrieved from https://agupubs.onlinelibrary.wiley.com/doi/abs/10.1029/94JA02577 doi: https://doi.org/10.1029/94JA02577

Fedder, J. A., Mobarry, C. M., & Lyon, J. G. (1991). Reconnection voltage as a function of imf clock angle. *Geophysical Research Letters*, *18*(6), 1047-1050. Retrieved from https://agupubs.onlinelibrary.wiley.com/doi/abs/10.1029/90GL02722 doi: https://doi.org/10.1029/90GL02722

Gershman, D. J., Slavin, J. A., Raines, J. M., Zurbuchen, T. H., Anderson, B. J., Korth, H., ... Solomon, S. C. (2013, November). Magnetic flux pileup and plasma depletion in Mercury's subsolar magnetosheath: PLASMA DEPLETION AT MERCURY. *Journal of Geophysical Research: Space Physics*, *118*(11), 7181–7199. Retrieved 2021-08-30, from http://doi.wiley.com/10.1002/2013JA019244 doi: 10.1002/2013JA019244

Glassmeier, K.-H., Grosser, J., Auster, U., Constantinescu, D., Narita, Y., & Stellmach, S. (2007, October). Electromagnetic Induction Effects and Dynamo Action in the Hermean System. *Space Science Reviews*, *132*(2-4), 511–527. Retrieved 2021-08-30, from http://link.springer.com/10.1007/s11214-007-9244-9 doi: 10.1007/s11214-007-9244-9

Gosling, J. T., Baker, D. N., Bame, S. J., Feldman, W. C., Zwickl, R. D., & Smith, E. J. (1985). North-south and dawn-dusk plasma asymmetries in the distant tail lobes: ISEE 3. *Journal of Geophysical Research*, *90*(A7), 6354. Retrieved 2021-08-30, from http://doi.wiley.com/10.1029/JA090iA07p06354 doi: 10.1029/JA090iA07p06354

Hauck, S. A., Margot, J.-L., Solomon, S. C., Phillips, R. J., Johnson, C. L., Lemoine, F. G., ... Zuber, M. T. (2013, June). The curious case of Mercury's internal structure: MERCURY'S INTERNAL STRUCTURE. *Journal of Geophysical Research: Planets*, *118*(6), 1204–1220. Retrieved 2021-08-31, from http://doi.wiley.com/10.1002/jgre.20091 doi: 10.1002/jgre.20091

Heyner, D., Nabert, C., Liebert, E., & Glassmeier, K. (2016, April). Concerning reconnectioninduction balance at the magnetopause of Mercury. *Journal of Geophysical Research: Space Physics*, *121*(4), 2935–2961. Retrieved 2021-08-30, from https://onlinelibrary.wiley.com/doi/abs/10.1002/2015JA021484 doi: 10.1002/2015JA021484

Hood, L., & Schubert, G. (1979). Inhibition of solar wind impingement on mercury by planetary induction currents. *Journal of Geophysical Research*, *84*(A6), 2641. Retrieved 2021-08-30, from http://doi.wiley.com/10.1029/JA084iA06p02641 doi: 10.1029/JA084iA06p02641

Imber, S. M., & Slavin, J. A. (2017). Messenger observations of magnetotail loading and unloading: Implications for substorms at mercury. *Journal of Geophysical Research: Space Physics*, *122*(11), 11,402-11,412. Retrieved from https://agupubs.onlinelibrary.wiley.com/doi/abs/10.1002/2017JA024332 doi: https://doi.org/10.1002/2017JA024332

James, M. K., Imber, S. M., Bunce, E. J., Yeoman, T. K., Lockwood, M., Owens, M. J., & Slavin, J. A. (2017, August). Interplanetary magnetic field prop-

erties and variability near Mercury's orbit: IMF AT MERCURY. *Journal of Geophysical Research: Space Physics*, *122*(8), 7907–7924. Retrieved 2021-08-30, from http://doi.wiley.com/10.1002/2017JA024435 doi: 10.1002/2017JA024435

Jia, X., Slavin, J. A., Gombosi, T. I., Daldorff, L. K. S., Toth, G., & Holst, B. (2015, June). Global MHD simulations of Mercury's magnetosphere with coupled planetary interior: Induction effect of the planetary conducting core on the global interaction. *Journal of Geophysical Research: Space Physics*, *120*(6), 4763–4775. Retrieved 2021-08-30, from https://onlinelibrary.wiley.com/doi/abs/10.1002/2015JA021143 doi: 10.1002/2015JA021143

Jia, X., Slavin, J. A., Poh, G., DiBraccio, G. A., Toth, G., Chen, Y., ... Gombosi, T. I. (2019, January). MESSENGER Observations and Global Simulations of Highly Compressed Magnetosphere Events at Mercury. *Journal of Geophysical Research: Space Physics*, *124*(1), 229–247. Retrieved 2021-08-30, from https://onlinelibrary.wiley.com/doi/abs/10.1029/2018JA026166 doi: 10.1029/2018JA026166

Johnson, C. L., Philpott, L. C., Anderson, B. J., Korth, H., Hauck, S. A., Heyner, D., ... Solomon, S. C. (2016, March). MESSENGER observations of induced magnetic fields in Mercury's core. *Geophysical Research Letters*, *43*(6), 2436–2444. Retrieved 2021-08-30, from https://onlinelibrary.wiley.com/doi/abs/10.1002/2015GL067370 doi: 10.1002/2015GL067370

Johnson, C. L., Purucker, M. E., Korth, H., Anderson, B. J., Winslow, R. M., Al Asad, M. M. H., ... Solomon, S. C. (2012, December). MESSENGER observations of Mercury's magnetic field structure: MERCURY'S MAGNETIC FIELD STRUCTURE. *Journal of Geophysical Research: Planets*, *117*(E12), n/a–n/a. Retrieved 2021-08-30, from http://doi.wiley.com/10.1029/2012JE004217 doi: 10.1029/2012JE004217

Katsura, T., Shimizu, H., Momoki, N., & Toh, H. (2021, January). Electromagnetic induction revealed by MESSENGER's vector magnetic data: The size of Mercury's core. *Icarus*, *354*, 114112. Retrieved 2021-08-30, from https://linkinghub.elsevier.com/retrieve/pii/S0019103520304577 doi: 10.1016/j.icarus.2020.114112

Kaymaz, Z., Siscoe, G. L., Luhmann, J. G., Lepping, R. P., & Russell, C. T. (1994). Interplanetary magnetic field control of magnetotail magnetic field geometry: Imp 8 observations. *Journal of Geophysical Research: Space Physics*, *99*(A6), 11113-11126. Retrieved from https://agupubs.onlinelibrary.wiley.com/doi/abs/10.1029/94JA00300 doi: https://doi.org/10.1029/94JA00300

Khurana, K. K., Walker, R. J., & Ogino, T. (1996). Magnetospheric convection in the presence of interplanetary magnetic field by : A conceptual model and simulations. *Journal of Geophysical Research: Space Physics*, *101*(A3), 4907-4916. Retrieved from https://agupubs.onlinelibrary.wiley.com/doi/abs/10.1029/95JA03673 doi: https://doi.org/10.1029/95JA03673

Luhmann, J. G., Walker, R. J., Russell, C. T., Crooker, N. U., Spreiter, J. R., & Stahara, S. S. (1984). Patterns of potential magnetic field merging sites on the dayside magnetopause. *Journal of Geophysical Research: Space Physics*, *89*(A3), 1739-1742. Retrieved from https://agupubs.onlinelibrary.wiley.com/doi/abs/10.1029/JA089iA03p01739 doi: https://doi.org/10.1029/JA089iA03p01739

Ness, N. F., Behannon, K. W., Lepping, R. P., Whang, Y. C., & Schatten, K. H. (1974, July). Magnetic Field Observations near Mercury: Preliminary Results from Mariner 10. *Science*, *185*(4146), 151–160. Retrieved 2021-08-31, from https://www.sciencemag.org/lookup/doi/10.1126/science.185.4146.151 doi: 10.1126/science.185.4146.151

Owen, C. J., Slavin, J. A., Richardson, I. G., Murphy, N., & Hynds, R. J. (1995). Average motion, structure and orientation of the distant magnetotail deter-

mined from remote sensing of the edge of the plasma sheet boundary layer with $E > 35$ keV ions. *Journal of Geophysical Research*, *100*(A1), 185. Retrieved 2021-08-30, from http://doi.wiley.com/10.1029/94JA02417 doi: 10.1029/94JA02417

Park, K. S., Ogino, T., & Walker, R. J. (2006). On the importance of antiparallel reconnection when the dipole tilt and IMF B_y are nonzero. *Journal of Geophysical Research*, *111*(A5), A05202. Retrieved 2021-08-30, from http://doi.wiley.com/10.1029/2004JA010972 doi: 10.1029/2004JA010972

Philpott, L. C., Johnson, C. L., Anderson, B. J., & Winslow, R. M. (2020). The shape of mercury's magnetopause: The picture from messenger magnetometer observations and future prospects for bepicolombo. *Journal of Geophysical Research: Space Physics*, *125*(5), e2019JA027544. Retrieved from https://agupubs.onlinelibrary.wiley.com/doi/abs/10.1029/2019JA027544 (e2019JA027544 10.1029/2019JA027544) doi: https://doi.org/10.1029/2019JA027544

Pitknen, T., Kullen, A., Cai, L., Park, J.-S., Vanhamki, H., Hamrin, M., ... Shi, Q. (2021, December). Asymmetry in the Earths magnetotail neutral sheet rotation due to IMF B_y sign? *Geoscience Letters*, *8*(1), 3. Retrieved 2021-08-30, from https://geoscienceletters.springeropen.com/articles/10.1186/s40562-020-00171-7 doi: 10.1186/s40562-020-00171-7

Poh, G., Slavin, J. A., Jia, X., Raines, J. M., Imber, S. M., Sun, W., ... Smith, A. W. (2017, January). Mercury's crosstail current sheet: Structure, Xline location and stress balance. *Geophysical Research Letters*, *44*(2), 678–686. Retrieved 2021-08-30, from https://onlinelibrary.wiley.com/doi/abs/10.1002/2016GL071612 doi: 10.1002/2016GL071612

Ramstad, R., Brain, D. A., Dong, Y., Espley, J., Halekas, J., & Jakosky, B. (2020, October). The global current systems of the Martian induced magnetosphere. *Nature Astronomy*, *4*(10), 979–985. Retrieved 2021-08-30, from http://www.nature.com/articles/s41550-020-1099-y doi: 10.1038/s41550-020-1099-y

Richer, E., Modolo, R., Chanteur, G. M., Hess, S., & Leblanc, F. (2012). A global hybrid model for mercury's interaction with the solar wind: Case study of the dipole representation. *Journal of Geophysical Research: Space Physics*, *117*(A10). Retrieved from https://agupubs.onlinelibrary.wiley.com/doi/abs/10.1029/2012JA017898 doi: https://doi.org/10.1029/2012JA017898

Romanelli, N., Bertucci, C., Gmez, D., & Mazelle, C. (2015, September). Dependence of the location of the Martian magnetic lobes on the interplanetary magnetic field direction: Observations from Mars Global Surveyor. *Journal of Geophysical Research: Space Physics*, *120*(9), 7737–7747. Retrieved 2021-08-31, from https://onlinelibrary.wiley.com/doi/abs/10.1002/2015JA021359 doi: 10.1002/2015JA021359

Romanelli, N., DiBraccio, G., Gershman, D., Le, G., Mazelle, C., Meziane, K., ... Espley, J. (2020). Upstream ultra-low frequency waves observed by messenger's magnetometer: Implications for particle acceleration at mercury's bow shock. *Geophysical Research Letters*, *47*(9), e2020GL087350. doi: 10.1029/2020GL087350

Romanelli, N., DiBraccio, G., Halekas, J., Dubinin, E., Gruesbeck, J., Espley, J., ... Luhmann, J. G. (2020, November). Variability of the Solar Wind Flow Asymmetry in the Martian Magnetosheath Observed by MAVEN. *Geophysical Research Letters*, *47*(22). Retrieved 2021-08-30, from https://onlinelibrary.wiley.com/doi/10.1029/2020GL090793 doi: 10.1029/2020GL090793

Romanelli, N., DiBraccio, G., Modolo, R., Leblanc, F., Espley, J., Gruesbeck, J., ... Jakosky, B. (2019, October). Recovery Timescales of the Dayside Martian Magnetosphere to IMF Variability. *Geophysical Research Letters*, *46*(20),

10977–10986. Retrieved 2021-08-31, from https://onlinelibrary.wiley.com/doi/10.1029/2019GL084151 doi: 10.1029/2019GL084151

Romanelli, N., & DiBraccio, G. A. (2021, November). Occurrence rate of ultra-low frequency waves in the foreshock of Mercury increases with heliocentric distance. *Nature Communications*, *12*, 6748. doi: 10.1038/s41467-021-26344-2

Romanelli, N., Gmez, D., Bertucci, C., & Delva, M. (2014, June). STEADY-STATE MAGNETOHYDRODYNAMIC FLOW AROUND AN UNMAGNETIZED CONDUCTING SPHERE. *The Astrophysical Journal*, *789*(1), 43. Retrieved 2021-08-31, from https://iopscience.iop.org/article/10.1088/0004-637X/789/1/43 doi: 10.1088/0004-637X/789/1/43

Romanelli, N., Modolo, R., Leblanc, F., Chaufray, J.-Y., Hess, S., Brain, D., ... Jakosky, B. (2018). Effects of the crustal magnetic fields and changes in the imf orientation on the magnetosphere of mars: Maven observations and lathys results. *Journal of Geophysical Research: Space Physics*, *123*(7), 5315-5333. Retrieved from https://agupubs.onlinelibrary.wiley.com/doi/abs/10.1029/2017JA025155 doi: https://doi.org/10.1029/2017JA025155

Rong, Z. J., Ding, Y., Slavin, J. A., Zhong, J., Poh, G., Sun, W. J., ... Shen, C. (2018, January). The Magnetic Field Structure of Mercury's Magnetotail. *Journal of Geophysical Research: Space Physics*, *123*(1), 548–566. Retrieved 2021-08-30, from https://onlinelibrary.wiley.com/doi/10.1002/2017JA024923 doi: 10.1002/2017JA024923

Saur, J., Neubauer, F. M., & Glassmeier, K.-H. (2010, May). Induced Magnetic Fields in Solar System Bodies. *Space Science Reviews*, *152*(1-4), 391–421. Retrieved 2021-08-30, from http://link.springer.com/10.1007/s11214-009-9581-y doi: 10.1007/s11214-009-9581-y

Sibeck, D. G., Siscoe, G. L., Slavin, J. A., Smith, E. J., Tsurutani, B. T., & Lepping, R. P. (1985). The distant magnetotail's response to a strong interplanetary magnetic field B $_{y}$: Twisting, flattening, and field line bending. *Journal of Geophysical Research*, *90*(A5), 4011. Retrieved 2021-08-30, from http://doi.wiley.com/10.1029/JA090iA05p04011 doi: 10.1029/JA090iA05p04011

Slavin, J., Owen, J., Connerney, J., & Christon, S. (1997, January). Mariner 10 observations of field-aligned currents at Mercury. *Planetary and Space Science*, *45*(1), 133–141. Retrieved 2021-08-30, from https://linkinghub.elsevier.com/retrieve/pii/S0032063396001043 doi: 10.1016/S0032-0633(96)00104-3

Slavin, J. A., Acuna, M. H., Anderson, B. J., Baker, D. N., Benna, M., Boardsen, S. A., ... Zurbuchen, T. H. (2009, May). MESSENGER Observations of Magnetic Reconnection in Mercury's Magnetosphere. *Science*, *324*(5927), 606–610. Retrieved 2021-09-02, from https://www.sciencemag.org/lookup/doi/10.1126/science.1172011 doi: 10.1126/science.1172011

Slavin, J. A., Anderson, B. J., Baker, D. N., Benna, M., Boardsen, S. A., Gold, R. E., ... Zurbuchen, T. H. (2012, January). MESSENGER and Mariner 10 flyby observations of magnetotail structure and dynamics at Mercury: MERCURY'S MAGNETOTAIL. *Journal of Geophysical Research: Space Physics*, *117*(A1). Retrieved 2021-08-30, from http://doi.wiley.com/10.1029/2011JA016900 doi: 10.1029/2011JA016900

Slavin, J. A., DiBraccio, G. A., Gershman, D. J., Imber, S. M., Poh, G. K., Raines, J. M., ... Solomon, S. C. (2014, October). MESSENGER observations of Mercury's dayside magnetosphere under extreme solar wind conditions. *Journal of Geophysical Research: Space Physics*, *119*(10), 8087–8116. Retrieved 2021-08-30, from http://doi.wiley.com/10.1002/2014JA020319 doi: 10.1002/2014JA020319

Slavin, J. A., & Holzer, R. E. (1981). Solar wind flow about the terrestrial planets 1. Modeling bow shock position and shape. *Journal of Geophysical Research*,

86(A13), 11401. Retrieved 2021-08-30, from http://doi.wiley.com/10.1029/JA086iA13p11401 doi: 10.1029/JA086iA13p11401

Slavin, J. A., Imber, S. M., & Raines, J. M. (2021). A dungey cycle in the life of mercury's magnetosphere. In *Magnetospheres in the solar system* (p. 535-556). American Geophysical Union (AGU). Retrieved from https://agupubs.onlinelibrary.wiley.com/doi/abs/10.1002/9781119815624.ch34 doi: https://doi.org/10.1002/9781119815624.ch34

Slavin, J. A., Middleton, H. R., Raines, J. M., Jia, X., Zhong, J., Sun, W., ... Mays, M. L. (2019, August). MESSENGER Observations of Disappearing Dayside Magnetosphere Events at Mercury. *Journal of Geophysical Research: Space Physics*, *124*(8), 6613–6635. Retrieved 2021-09-01, from https://onlinelibrary.wiley.com/doi/10.1029/2019JA026892 doi: 10.1029/2019JA026892

Smith, D. E., Zuber, M. T., Phillips, R. J., Solomon, S. C., Hauck, S. A., Lemoine, F. G., ... Taylor, A. H. (2012, April). Gravity Field and Internal Structure of Mercury from MESSENGER. *Science*, *336*(6078), 214–217. Retrieved 2021-08-31, from https://www.sciencemag.org/lookup/doi/10.1126/science.1218809 doi: 10.1126/science.1218809

Solomon, S. C., McNutt, R. L., Gold, R. E., & Domingue, D. L. (2007, August). MESSENGER Mission Overview. *Space Science Reviews*, *131*(1-4), 3–39. Retrieved 2021-09-01, from http://link.springer.com/10.1007/s11214-007-9247-6 doi: 10.1007/s11214-007-9247-6

Sun, W., Dewey, R. M., Aizawa, S., Huang, J., Slavin, J. A., Fu, S., & Bowers, C. F. (2021). Review of Mercurys Dynamic Magnetosphere: Post-MESSENGER Era and Comparative Magnetospheres. *https://arxiv.org/abs/2103.16778*, 97.

Tenfjord, P., stgaard, N., Snekvik, K., Laundal, K. M., Reistad, J. P., Haaland, S., & Milan, S. E. (2015, November). How the IMF B_y induces a B_y component in the closed magnetosphere and how it leads to asymmetric currents and convection patterns in the two hemispheres. *Journal of Geophysical Research: Space Physics*, *120*(11), 9368–9384. Retrieved 2021-08-30, from https://onlinelibrary.wiley.com/doi/10.1002/2015JA021579 doi: 10.1002/2015JA021579

Tsyganenko, N. A., Andreeva, V. A., & Gordeev, E. I. (2015). Internally and externally induced deformations of the magnetospheric equatorial current as inferred from spacecraft data. *Annales Geophysicae*, *33*(1), 1–11. Retrieved from https://angeo.copernicus.org/articles/33/1/2015/ doi: 10.5194/angeo-33-1-2015

Tsyganenko, N. A., Karlsson, S. B. P., Kokubun, S., Yamamoto, T., Lazarus, A. J., Ogilvie, K. W., ... Slavin, J. A. (1998, April). Global configuration of the magnetotail current sheet as derived from Geotail, Wind, IMP 8 and ISEE 1/2 data. *Journal of Geophysical Research: Space Physics*, *103*(A4), 6827–6841. Retrieved 2021-08-30, from http://doi.wiley.com/10.1029/97JA03621 doi: 10.1029/97JA03621

Wardinski, I., Langlais, B., & Thbault, E. (2019, August). Correlated TimeVarying Magnetic Fields and the Core Size of Mercury. *Journal of Geophysical Research: Planets*, *124*(8), 2178–2197. Retrieved 2021-08-30, from https://onlinelibrary.wiley.com/doi/abs/10.1029/2018JE005835 doi: 10.1029/2018JE005835

Wing, S., Newell, P. T., Sibeck, D. G., & Baker, K. B. (1995, August). A large statistical study of the entry of interplanetary magnetic field Y-component into the magnetosphere. *Geophysical Research Letters*, *22*(16), 2083–2086. Retrieved 2021-08-30, from http://doi.wiley.com/10.1029/95GL02261 doi: 10.1029/95GL02261

Winslow, R. M., Lugaz, N., Philpott, L., Farrugia, C. J., Johnson, C. L., Anderson, B. J., ... Asad, M. A. (2020, February). Observations of Extreme ICME

Ram Pressure Compressing Mercurys Dayside Magnetosphere to the Surface. *The Astrophysical Journal*, *889*(2), 184. Retrieved 2021-08-30, from https://iopscience.iop.org/article/10.3847/1538-4357/ab6170 doi: 10.3847/1538-4357/ab6170

Xiao, S., Zhang, T., Ge, Y., Wang, G., Baumjohann, W., & Nakamura, R. (2016, February). A statistical study on the shape and position of the magnetotail neutral sheet. *Annales Geophysicae*, *34*(2), 303–311. Retrieved 2021-08-30, from https://angeo.copernicus.org/articles/34/303/2016/ doi: 10.5194/angeo-34-303-2016

Zhong, J., Wan, W. X., Slavin, J. A., Wei, Y., Lin, R. L., Chai, L. H., ... Han, X. H. (2015). Mercury's three-dimensional asymmetric magnetopause. *Journal of Geophysical Research: Space Physics*, *120*(9), 7658-7671. Retrieved from https://agupubs.onlinelibrary.wiley.com/doi/abs/10.1002/2015JA021425 doi: https://doi.org/10.1002/2015JA021425

Zhong, J., Wan, W. X., Wei, Y., Slavin, J. A., Raines, J. M., Rong, Z. J., ... Han, X. H. (2015, December). Compressibility of Mercury's dayside magnetosphere. *Geophysical Research Letters*, *42*(23). Retrieved 2021-08-30, from https://onlinelibrary.wiley.com/doi/abs/10.1002/2015GL067063 doi: 10.1002/2015GL067063

Zurbuchen, T., Koehn, P., Fisk, L., Gombosi, T., Gloeckler, G., & Kabin, K. (2004, January). On the space environment of Mercury. *Advances in Space Research*, *33*(11), 1884–1889. Retrieved 2021-08-30, from https://linkinghub.elsevier.com/retrieve/pii/S0273117704000110 doi: 10.1016/j.asr.2003.04.048